















RESEARCH ARTICLE | JANUARY 23 2023

# Controlling interface anisotropy in CoFeB/MgO/HfO<sub>2</sub> using dusting layers and magneto-ionic gating

Special Collection: [Magneto-ionic and electrostatic gating of magnetism: Phenomena and devices](#)

T. Bhatnagar-Schöffmann ; A. Kovács ; R. Pachat ; D. Ourdani ; A. Lamperti ; M.-A. Syskaki ;  
 T. da Câmara Santa Clara Gomes; Y. Roussigné ; S. Ono ; J. Langer ; M. Cherif ;  
 R. E. Dunin-Borkowski; P. Schöffmann ; D. Ravelosona; M. Belmeguenai ; A. Solignac;  
 L. Herrera Diez  



Appl. Phys. Lett. 122, 042402 (2023)

<https://doi.org/10.1063/5.0132870>

Instruments for Advanced Science

- Knowledge
- Experience
- Expertise

Click to view our product catalogue

Contact Hiden Analytical for further details:

[www.HidenAnalytical.com](http://www.HidenAnalytical.com)

[info@hiden.co.uk](mailto:info@hiden.co.uk)

**Gas Analysis**

- dynamic measurement of reaction gas streams
- catalysis and thermal analysis
- molecular beam studies
- dissolved species probes
- fermentation, environmental and ecological studies

**Surface Science**

- UHV/TPD
- SIMS
- end point detection in ion beam etch
- elemental imaging - surface mapping

**Plasma Diagnostics**

- plasma source characterization
- etch and deposition process reaction kinetic studies
- analysis of neutral and radical species

**Vacuum Analysis**

- partial pressure measurement and control of process gases
- reactive sputter process control
- vacuum diagnostics
- vacuum coating process monitoring

# Controlling interface anisotropy in CoFeB/MgO/HfO<sub>2</sub> using dusting layers and magneto-ionic gating

Cite as: Appl. Phys. Lett. **122**, 042402 (2023); doi: [10.1063/5.0132870](https://doi.org/10.1063/5.0132870)

Submitted: 31 October 2022 · Accepted: 4 January 2023 ·

Published Online: 23 January 2023



View Online



Export Citation



CrossMark

T. Bhatnagar-Schöffmann,<sup>1</sup> A. Kovács,<sup>2</sup> R. Pachat,<sup>1</sup> D. Ourdani,<sup>3</sup> A. Lamperti,<sup>4</sup> M.-A. Syskaki,<sup>5</sup> T. da Câmara Santa Clara Gomes,<sup>6</sup> Y. Roussigné,<sup>3</sup> S. Ono,<sup>7</sup> J. Langer,<sup>5</sup> M. Cherif,<sup>3</sup> R. E. Dunin-Borkowski,<sup>2</sup> P. Schöffmann,<sup>8</sup> D. Ravelosona,<sup>9</sup> M. Belmeguenai,<sup>3</sup> A. Solignac,<sup>10</sup> and L. Herrera Diez<sup>1,a)</sup>

## AFFILIATIONS

<sup>1</sup>Centre de Nanosciences et de Nanotechnologies, CNRS, Université Paris-Saclay, 91120 Palaiseau, France

<sup>2</sup>Forschungszentrum Jülich GmbH, Ernst Ruska-Centre for Microscopy and Spectroscopy with Electrons and Peter Grünberg Institute (PGI-5), 52425 Jülich, Germany

<sup>3</sup>Laboratoire des Sciences des Procédés et des Matériaux, CNRS-UPR 3407, Université Sorbonne Paris Nord, 93430 Villetaneuse, France

<sup>4</sup>CNR-IMM, Agrate Unit, Via C. Olivetti 2, 20864 Agrate Brianza (MB), Italy

<sup>5</sup>Singulus Technologies AG, Hanauer Landstrasse 103, 63796 Kahl am Main, Germany

<sup>6</sup>Unité Mixte de Physique CNRS/Thales, Université Paris-Saclay, 91767 Palaiseau, France

<sup>7</sup>Central Research Institute of Electric Power Industry, Yokosuka, Kanagawa 240-0196, Japan

<sup>8</sup>Synchrotron SOLEIL, L'Orme des Merisiers, 91190 Saint-Aubin, France

<sup>9</sup>Spin-Ion Technologies, C2N, 10 Boulevard Thomas Gobert, 91120 Palaiseau, France

<sup>10</sup>SPEC, CEA, CNRS, Université Paris-Saclay, CEA Saclay, 91191 Gif-sur-Yvette Cedex, France

**Note:** This paper is part of the APL Special Collection on Magneto-ionic and electrostatic gating of magnetism: Phenomena and devices.

<sup>a)</sup>Author to whom correspondence should be addressed: [liza.herrera-diez@c2n.upsaclay.fr](mailto:liza.herrera-diez@c2n.upsaclay.fr)

## ABSTRACT

In this work, we present the magneto-ionic response to ionic liquid gating in Ta/CoFeB/MgO/HfO<sub>2</sub> stacks, where heavy metal dusting layers of Ta, W, and Pt are inserted at the Ta/CoFeB and CoFeB/MgO interfaces. Dusting layers of W inserted at the Ta/CoFeB interface increase perpendicular magnetic anisotropy (PMA) by more than 50%, while no significant changes are seen for Pt. In these samples, gating cannot break the PMA seeded at the CoFeB/MgO interface, only relatively small changes in the coercivity can be induced, about 20% for Ta and Pt and 6% for W. At the CoFeB/MgO interface, a significant quenching of the magnetization is seen when W and Ta dusting layers are inserted, which remains unchanged after gating, suggesting a critical deterioration of the CoFeB. In contrast, Pt dusting layers result in an in-plane anisotropy that can be reversibly converted to PMA through magneto-ionic gating while preserving the polycrystalline structure of the MgO layer. This shows that dusting layers can be effectively used not only to engineer magnetic properties in multilayers but also to strongly modify their magneto-ionic performance.

Published under an exclusive license by AIP Publishing. <https://doi.org/10.1063/5.0132870>

Electric field control of magnetism in nanostructured systems constitutes a solid route toward reducing power consumption in novel memory architectures. Both electrostatic and magneto-ionic effects have shown to greatly modify parameters like the magnetic anisotropy and the Dzyaloshinskii–Moriya interaction (DMI), leading to a very efficient control of domain wall dynamics and skyrmion motion.<sup>1–8</sup> Magneto-ionics is particularly attractive for low-power applications

since it provides nonvolatile changes in the magnetic states unlike charge effects, which need the constant application of a gate voltage. Significant advances have been recently made in magneto-ionics not only in ferromagnetic systems but also in ferrimagnets and synthetic antiferromagnets where large modulations of the magnetic compensation temperature and magnetic domain wall velocity have been observed.<sup>9,10</sup>

A key aspect in the development of magneto-ionic functionalities in spintronics devices is reaching a deep understanding of the ionic effects induced by the gate voltage. The choice of the oxide at the interface with the magnetic material has been shown to determine important aspects of the device performance such as the magnetic states that are accessible (in-plane/perpendicular anisotropy), stability of the non-volatile states, and reversibility.<sup>11</sup> Moreover, the degree of gate-voltage induced oxidation in the magnetic material can define different magneto-ionic regimes with marked differences in reversibility in the same device.<sup>6</sup> This shows the complexity of the magneto-ionic mechanisms, and interface engineering can play a key role in the design of optimized materials and devices for magneto-ionics.

The insertion of dusting layers in nanostructured magnetic stacks is an efficient strategy used in spintronics materials development to fine-tune properties, such as tunneling magnetoresistance (TMR), perpendicular magnetic anisotropy (PMA), and DMI.<sup>12–14</sup> On the other hand, devices containing CoFeB/MgO interfaces are of great technological relevance, since MgO allows for high tunneling magnetoresistance and PMA.<sup>15</sup> Therefore, it is of considerable interest to investigate the magneto-ionic behavior in systems with tunable Ta/CoFeB and CoFeB/MgO interfaces. In this work, we study the impact of dusting layers of Pt, W, and Ta inserted at the CoFeB/MgO and Ta/CoFeB interfaces in Ta/CoFeB/MgO/HfO<sub>2</sub> stacks on their magnetic and magneto-ionic properties. We reveal a strong dependence of interfacial magnetic anisotropy and magnetization on the composition and position of the dusting layers in the as-grown stacks and in the magneto-ionic response, which is also intimately related to the composition of the interfaces.

Magnetic stacks with the configuration Ta(5 nm)/(Y)/CoFeB(1 nm)/(X)/MgO(2 nm)/HfO<sub>2</sub>(3 nm) were deposited on thermally oxidized Si wafer substrates at room temperature. The inserted dusting layers of Pt, W, and Ta have a nominal thickness of 0.08 nm for W and Ta and 0.09 nm for Pt (see the [supplementary material](#)). The metallic layers (CoFeB, Pt, W, and Ta) were deposited by DC sputtering, and MgO and HfO<sub>2</sub> were deposited by RF sputtering. The base pressure of the sputtering system was  $1 \times 10^{-7}$  mbar, and the Ar pressure was kept at  $5 \times 10^{-3}$  mbar. The CoFeB composition is Co<sub>40</sub>Fe<sub>40</sub>B<sub>20</sub>. Ionic liquid (IL) gating is implemented by adding the ionic liquid 1-ethyl-3-methylimidazolium bis(trifluoromethanesulfonyl) imide [EMI]<sup>+</sup>[TFSI]<sup>−</sup> to the surface of the magnetic stacks.<sup>16</sup> A glass plate coated with indium tin oxide (ITO) is used as a counter electrode, which is placed on top of the IL. **Figure 1** shows a detailed depiction of the IL gating device. The size of the area exposed to electric fields is about 0.25 cm<sup>2</sup>, all measurements are conducted at room temperature, and all anomalous Hall effect (AHE) hysteresis loops were measured at zero gate voltage, exploiting the non-volatility of the magneto-ionic effects.

**Figure 2** shows vibrating sample magnetometry (VSM) measurements with magnetic fields (a) in the plane of the sample and along its (b) out-of-plane direction at 300 K, for all the as-grown samples in this study. The values of the saturation magnetization ( $M_s$ ) and the effective magnetic anisotropy constant ( $K_{eff}$ ) extracted from these measurements are plotted in **Fig. 2(c)** as a function of the interface composition. The ferromagnetic nature of the CoFeB layers is verified in all samples except for those where W is present at the CoFeB/MgO interface ( $X = W$  and  $X,Y = W$ ), where magnetization is reduced to values below the sensitivity limit of the VSM, indicating a critical

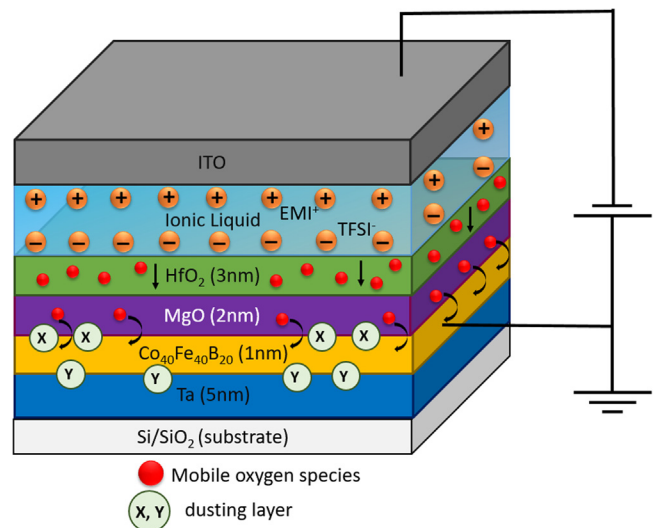


**FIG. 1.** Schematics of a magneto-ionic device containing an ionic liquid gate. Dusting layers are inserted at the Ta/CoFeB and CoFeB/MgO interfaces, indicated as Y and X, respectively.

degradation of the CoFeB. Reports in the literature show that sputtering W using Ar-gas can result in a higher degree of intermixing of W and CoFeB, leading to larger stress and more defects in CoFeB,<sup>17</sup> which can be at the origin of the severe degradation of magnetization in our samples. A significant magnetization quenching is also observed for the samples where Ta is present at the CoFeB/MgO interface ( $X,Y = Ta$ ); however, the sample still remains ferromagnetic. Intermixing between the dusting layer and CoFeB may be also at play for  $X = Ta$ . Studies in the literature have reported the presence of a 0.5 nm thick magnetic dead layer in MgO/CoFeB/Ta and no signature of a dead layer for Ta/CoFeB/MgO,<sup>15</sup> which is in agreement with our results and shows the importance of interface engineering.

For samples where  $Y = W$ , the effective perpendicular anisotropy increases by more than 50% with respect to samples where  $Y = Ta$  (no dusting layer), going from  $K_{eff} = 1.6 \times 10^5$  to  $2.5 \times 10^5$  J m<sup>−3</sup>. Intercalating W layers at the Ta/CoFeB interface has shown to increase PMA after annealing,<sup>18</sup> our observations show that it can also be the case in nonannealed systems and using only dusting layers of 0.08 nm.  $K_{eff}$  in samples where  $Y = Pt$  shows no significant difference with respect to samples where  $Y = Ta$ . However, when Pt dusting layers are in positions X and X,Y, the magnetic anisotropy is in-plane (negative  $K_{eff}$ ), although samples where  $X = Pt$  are significantly closer to the spin-reorientation transition (SRT).

The magneto-ionic response measured by AHE hysteresis loops for samples where  $Y = Ta$ , W, or Pt is shown in **Figs. 3(a)–3(c)**, while (i) shows a drawing of the AHE measurement geometry. Gate voltages of  $-3.5$  and  $+4$  V were applied for 600 and 180 s, respectively, to all three samples. Only a modest and reversible variation of the coercivity can be obtained through gating, about 20% for  $Y = Ta$  and Pt and about 6% for  $Y = W$  (see the [supplementary material](#)). The reduced performance of the sample where  $Y = W$  is attributed to its higher anisotropy. The SRT from PMA to in-plane anisotropy cannot be observed within the gate voltage range available, by moving neither

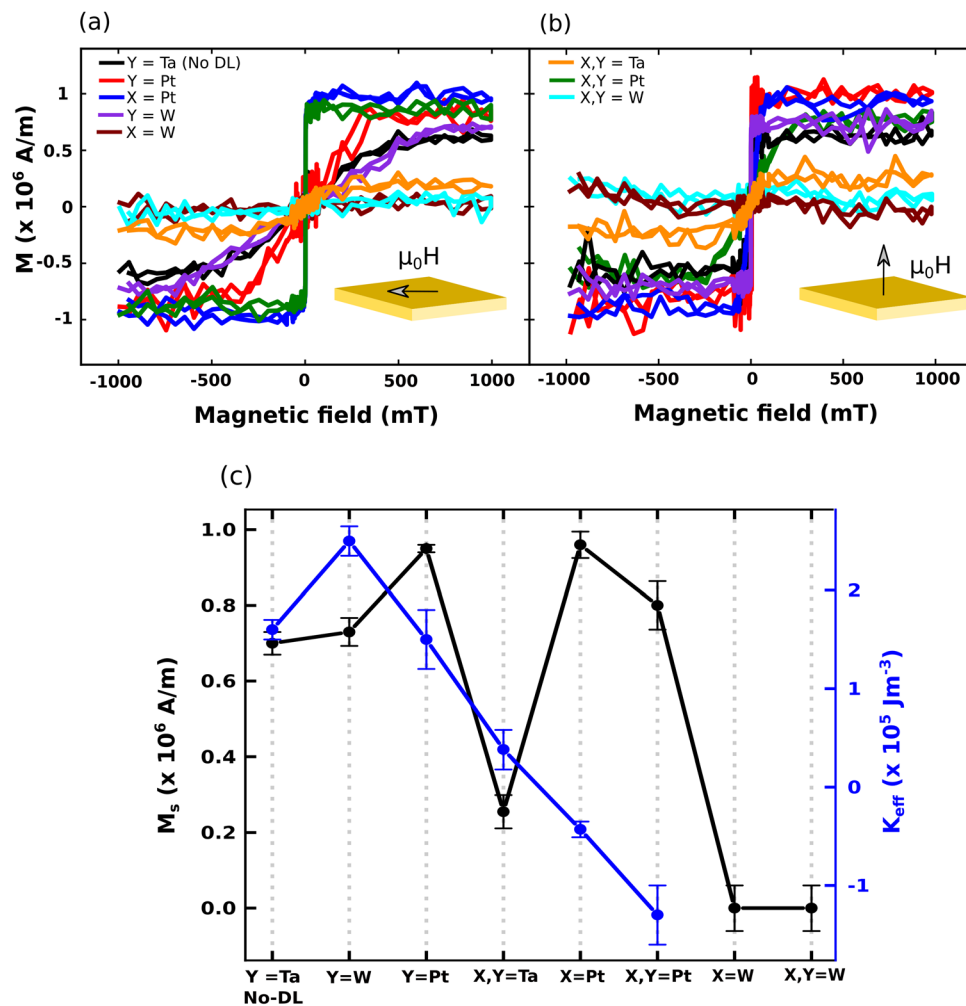


**FIG. 2.** (a) In-plane and (b) out-of-plane VSM measurements of as-grown samples. (c) Variation in saturation magnetization ( $M_s$ ) and in the effective anisotropy constant ( $K_{eff}$ ) as a function of interface composition.

toward the underoxidized regime, which is compatible with the irreversible effects seen in Co/MgO/ZrO<sub>2</sub>,<sup>11</sup> nor to the overoxidized regime. This shows that the dominant PMA contribution coming from the CoFeB/MgO cannot be suppressed by gating in these samples, since the as-grown  $K_{eff}$  values are relatively far from the SRT. It is worth noting that the coercivity values for Y = W and Pt are significantly lower than in the Y = Ta sample. As  $K_{eff}$  does not decrease, a reduction in coercivity could be attributed to a higher degree of disorder at the Ta/CoFeB interface when dusting layers are present, which could promote the nucleation of reverse domains at lower fields.

Decoupling the CoFeB/MgO interface through dusting layers can be a strategy to approach the SRT in the as-grown state and achieve an efficient magneto-ionic performance showing both a SRT and reversibility. Figures 3(d)–3(f) show AHE hysteresis loops for X = Ta, W, and Pt, respectively. As previously discussed, all samples exhibit a loss of PMA; however, the samples where X = Ta, W show a serious deterioration in their magnetic properties, and gating does not induce any

effects [the same applies to Fig. 3(g)]. In contrast, the sample where X = Pt shows a relatively high magnetic moment and an in-plane anisotropy close to the SRT. In this sample, the conditions are given for magneto-ionic gating to reversibly induce an SRT, as can be seen in Fig. 3(f), obtaining also good cyclability (see the supplementary material). It was shown in Fig. 2(c) that for samples where X, Y = Pt, in-plane anisotropy is significantly farther away from the SRT than the X = Pt sample. This can limit the effects of magneto-ionic gating in the gate voltage range allowed in our devices, which is verified in the measurements presented in Fig. 3(h). However, the significant increase in the in-plane  $K_{eff}$  in the X, Y = Pt sample compared to the X = Pt sample is intuitively unexpected, considering that the Y = Pt sample has a relatively high PMA and that the X = Pt sample is close to the SRT. A possible interpretation could be made considering the potential diffusion of the atoms of the bottom Pt buffer layer into the CoFeB layer and up to the CoFeB/MgO interface, which, already containing a Pt dusting layer, may contribute to making conditions harder

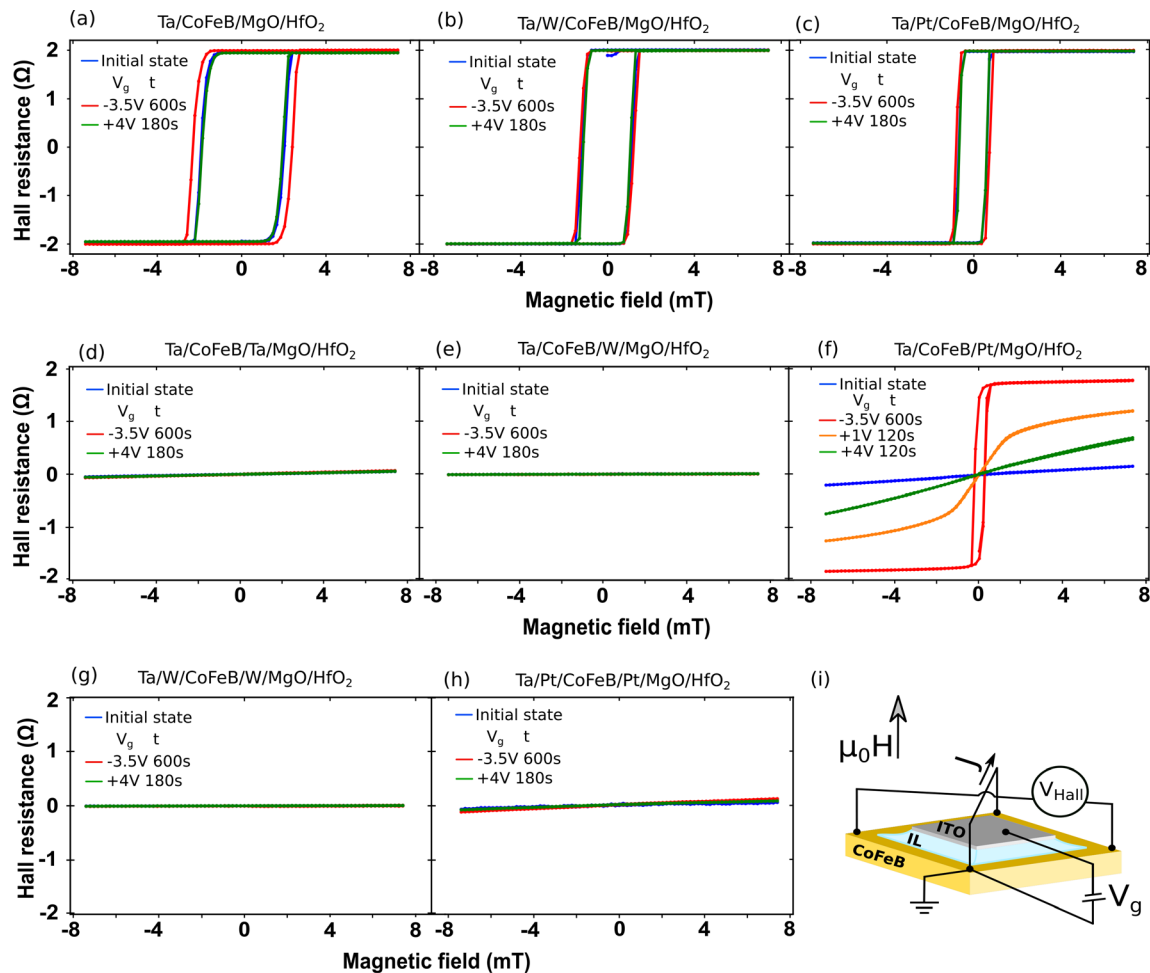


**FIG. 3.** AHE hysteresis loops for Ta/Y/CoFeB/MgO/HfO<sub>2</sub> stacks with (a) Y = Ta (no dusting layer, directly grown on Ta), (b) Y = W, and (c) Y = Pt, and Ta/CoFeB/X/MgO/HfO<sub>2</sub> stacks with (d) X = Ta, (e) X = W, and (f) X = Pt. Panels (g) and (h) show hysteresis loops for the case when both X and Y = W and X and Y = Pt, respectively. In all configurations, Ta is used as a buffer layer. A schematic of the device used for AHE experiments is shown in (i).

for the development of PMA, for example by blocking the interaction between oxygen species and Co and Fe atoms. This consideration is made after observing that applying gate voltages to a sample of Ta/CoFeB/Pt/MgO where the Pt layer is 1 nm thick (see the [supplementary material](#)), no magneto-ionic effects are observed due to an excess of Pt atoms at the interface.

Previous studies have shown that in Co/HfO<sub>2</sub>, a negative gate voltage applied to the ITO electrode induces oxidation in the Co layer, which leads to an SRT from in-plane anisotropy to PMA.<sup>5</sup> This has been attributed to the migration of oxygen species from the HfO<sub>2</sub> toward the ferromagnetic layer under the action of the applied voltage. A voltage controlled oxidation and SRT upon negative gate voltage exposure have also been observed in Fe rich CoFeB alloys (Co<sub>20</sub>Fe<sub>60</sub>B<sub>20</sub>/HfO<sub>2</sub>).<sup>6</sup> In these two systems, the transition from under-oxidized with in-plane anisotropy to optimum oxidation with PMA was found to be irreversible. Studies have also reported that applying a negative voltage to the top electrode in a Co/MgO/ZrO<sub>2</sub> based device enhances PMA also in a nonvolatile but irreversible way.<sup>11</sup> In this last

case, the MgO layer is created by the natural oxidation of a sub-nm layer of Mg inserted at the interface, which may not present an optimum interfacial oxidation before the application of the voltage, and a first oxidation through gating may induce an irreversible transition to PMA, as observed in Co/HfO<sub>2</sub><sup>5</sup> and CoFeB/HfO<sub>2</sub>.<sup>6</sup> In the present study, the MgO layer is 2 nm thick and is sputtered *in situ* from an MgO target onto the CoFeB layer. Figure 4 shows bright-field scanning transmission electron microscopy (TEM) images of an X = Pt sample (a) before and (b) after gate voltage application. The as-grown sample, as shown earlier, has in-plane magnetic anisotropy, while the sample from Fig. 4(b) experienced seven cycles of application of -3.5 V/+4 V, before being set to a final PMA state (see the [supplementary material](#)). In both cases, the MgO barrier shows a high degree of crystallinity that is not affected by the application of the gate voltage, while the HfO<sub>2</sub> layer remains amorphous. This means that oxygen species coming from the HfO<sub>2</sub> layer can reversibly diffuse across 2 nm of MgO without interacting strongly with the Mg atoms, most likely using the grain boundaries of the polycrystalline MgO layer as ion conduction



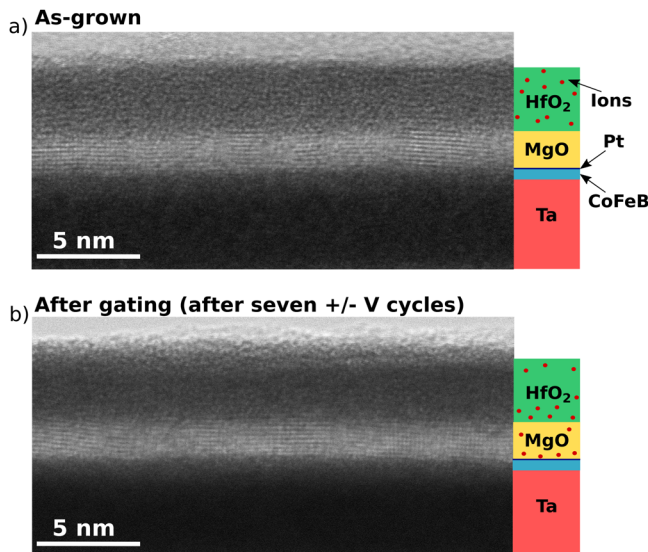


**FIG. 4.** Bright-field scanning TEM images of Ta/CoFeB/Pt(0.09)/MgO/HfO<sub>2</sub> stacks (a) as-grown and (b) after seven cycles of application of  $-3.5$  V/ $+4$  V gate voltages. The final magnetic anisotropy state of the sample is PMA.

channels, a concept already proposed for other magneto-ionic systems.<sup>19</sup> The structural order observed in MgO in our samples may be a determining factor in the magneto-ionic reversibility observed in this system, compared to the irreversible effects seen for MgO layers obtained by natural oxidation,<sup>11</sup> potentially containing a higher degree of disorder. In the case of  $X = \text{Pt}$  samples, the presence of Pt atoms at the CoFeB/MgO interface may also regulate the flow of oxygen species beyond the interface and into the CoFeB, which could serve as a means to control the ion penetration and, in turn, contribute to avoiding irreversible effects.

The stability of the PMA and in-plane anisotropy states obtained after gate voltage application for  $X = \text{Pt}$  samples was also examined. AHE hysteresis loops were recorded right after the application of a

gate voltage of either  $-3.5$  V for 600 s or  $+4$  V for 360 s (day 1) and everyday for the following seven days as shown in Figs. 5(a) and 5(b), respectively. It is observed that the PMA induced through magneto-ionic gating is conserved throughout the test period, while the gate-induced in-plane anisotropy state evolves significantly within the same time period. This effect is thought to be associated with a spontaneous re-absorption of oxygen species coming from the atmosphere after gating with positive voltages. Interestingly, the as-grown samples are very stable in air, and they do not develop PMA spontaneously. This evolution happens only in samples that have been switched first to a PMA state and subsequently reverted back to an in-plane state by the action of a positive gate voltage. This suggests that during the first application of negative gate voltages, ionic conduction channels are formed, which may allow for oxygen species to reenter the sample after the positive voltage is switched off, slowly driving the magnetic state back to PMA.

In conclusion, we have systematically studied the influence of interface engineering on magnetic anisotropy and magneto-ionics through the insertion of dusting layers of Ta, W, and Pt in Ta/CoFeB/MgO/HfO<sub>2</sub> layers at the Ta/CoFeB and CoFeB/MgO interfaces. We observed an important degradation of the magnetic properties in samples where  $X = \text{Ta}$  or W (including  $X, Y = \text{W}$ ), and no dependence on the gate voltage. In samples where  $Y = \text{Ta}$ , W, and Pt, PMA is observed in all cases, highlighting the dominant contribution from the CoFeB/MgO interface to PMA. In these samples, only a relatively small modulation of the coercivity was observed, as the SRT was out of the range of the gate voltages applied. The sample where  $X = \text{Pt}$  presents optimum properties for magneto-ionics, as it has an in-plane anisotropy that can be driven across the SRT into a nonvolatile PMA state using a gate voltage. The gating effects are reversible and coexist with a high quality polycrystalline MgO layer. We also showed that while the gate-voltage induced PMA state is conserved over eight days after the application of the gate voltage, the in-plane anisotropy state achieved by applying positive gate voltages evolves significantly, reverting back toward the PMA state. These results show the importance of interface engineering for the design of efficient magneto-ionic materials for spintronics.

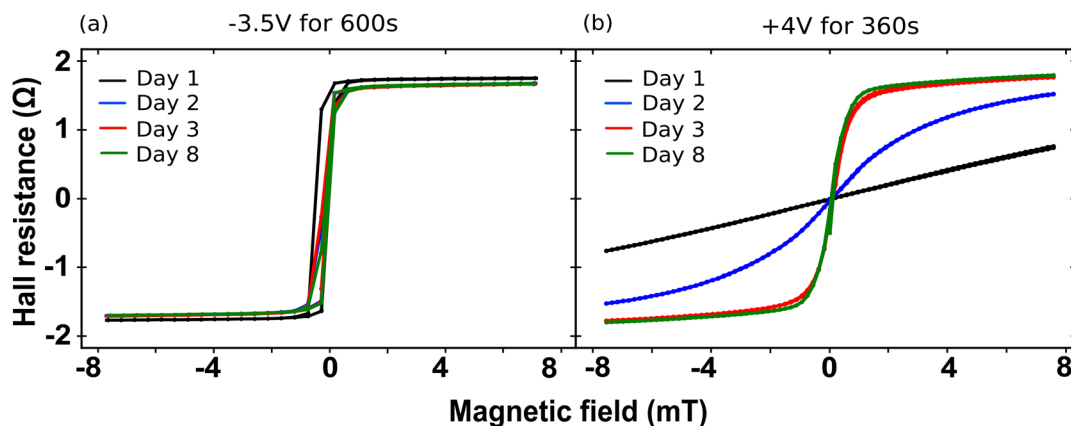


**FIG. 5.** AHE hysteresis loops recorded for a Ta/CoFeB/Pt(0.09)/MgO/HfO<sub>2</sub> sample over a span of 8 days, to examine the stability of (a) the PMA state and (b) the in-plane anisotropy state after applying gate voltages of  $-3.5$  V for 600 s and  $+4$  V for 360 s, respectively.

See the [supplementary material](#) for a discussion on the difference in the thickness of the dusting layers used in this work, and AHE plots for  $Y = \text{Pt}$  and  $W$  in a smaller scale ( $\pm 2 \text{ mT}$ ) to better see the changes in coercivity. We also include for  $\text{Ta/CoFeB/Pt}(0.09)/\text{MgO/HfO}_2$ : remanence reversibility cycles, AHE plots showing the behavior under gate voltages down to  $-1 \text{ V}$ , and the AHE plots corresponding to the samples measured by TEM. We also show the magneto-ionic response of a stack with a  $1 \text{ nm}$  thick  $\text{Pt}$  layer at position X.

We acknowledge financial support from the European Union H2020 Program (MSCA ITN 860060) and the French National Research Agency (JCJC SplaSy and Labex NanoSaclay, reference: ANR-10-LABX-0035). We also acknowledge support from the program PHC Sakura, the JSPS KAKENHI Grant (No. 20H05304), and European Union's Horizon 2020 Research and Innovation Program (Grant No. 823717), project "ESTEEM3" for access to TEM experiments.

## AUTHOR DECLARATIONS

### Conflict of Interest

The authors have no conflicts to disclose.

### Author Contributions

**Tanvi Bhatnagar-Schoeffmann:** Data curation (lead); Formal analysis (lead); Investigation (lead); Methodology (lead); Writing – original draft (lead); Writing – review & editing (lead). **Juergen Langer:** Methodology (supporting); Resources (supporting); Writing – review & editing (supporting). **Salim-Mourad Chérif:** Methodology (supporting); Resources (supporting). **Rafal Dunin-Borkowski:** Methodology (supporting); Resources (supporting); Writing – review & editing (supporting). **Patrick Schöffmann:** Data curation (supporting); Methodology (supporting); Resources (supporting); Writing – review & editing (supporting). **Dafine Ravelosona:** Methodology (supporting); Resources (supporting); Writing – review & editing (supporting). **Mohamed Belmeguenai:** Data curation (supporting); Formal analysis (supporting); Methodology (supporting); Resources (supporting); Writing – review & editing (supporting). **Aurelie Solignac:** Conceptualization (supporting); Data curation (supporting); Formal analysis (supporting); Methodology (supporting); Project administration (supporting); Supervision (supporting); Writing – review & editing (supporting). **Liza Herrera Diez:** Conceptualization (lead); Data curation (supporting); Formal analysis (supporting); Funding acquisition (lead); Investigation (equal); Methodology (lead); Project administration (lead); Resources (lead); Supervision (lead); Writing – original draft (equal); Writing – review & editing (equal). **András Kovács:** Data curation (supporting); Formal analysis (supporting); Investigation (supporting); Methodology (supporting); Writing – review & editing (equal). **Rohit Pachat:** Investigation (supporting); Methodology (supporting). **Djoudi Ourdani:** Data curation (supporting); Formal analysis (supporting); Investigation (supporting); Methodology (supporting); Writing – review & editing (supporting). **Alessio Lamperti:** Data curation (supporting); Formal analysis (supporting); Investigation (supporting); Methodology (supporting); Writing – review & editing (supporting). **Maria-Andromachi Syskaki:** Investigation (supporting); Methodology (supporting); Resources (supporting); Writing – review & editing (supporting). **Tristan da Câmara Santa Clara Gomes:** Data curation

(supporting); Formal analysis (supporting); Writing – review & editing (supporting). **Yves Roussigné:** Data curation (supporting); Formal analysis (supporting); Methodology (supporting); Writing – review & editing (supporting). **Shimpei Ono:** Methodology (supporting); Resources (supporting); Writing – review & editing (supporting).

## DATA AVAILABILITY

The data that support the findings of this study are available from the corresponding author upon reasonable request.

## REFERENCES

- 1A. Bernard-Mantel, L. Herrera-Diez, L. Ranno, S. Pizzini, J. Vogel, D. Givord, S. Auffret, O. Boulle, I. M. Miron, and G. Gaudin, "Electric-field control of domain wall nucleation and pinning in a metallic ferromagnet," *Appl. Phys. Lett.* **102**, 122406 (2013).
- 2Y. T. Liu, S. Ono, and G. Agnus, "Electric field controlled domain wall dynamics and magnetic easy axis switching in liquid gated  $\text{CoFeB/MgO}$  films," *J. Appl. Phys.* **122**, 133907 (2017).
- 3M. Schott, A. Bernard-Mantel, L. Ranno, S. Pizzini, J. Vogel, H. Béa, C. Baraduc, S. Auffret, G. Gaudin, and D. Givord, "The skyrmion switch: Turning magnetic skyrmion bubbles on and off with an electric field," *Nano Lett.* **17**, 3006–3012 (2017).
- 4T. Srivastava, M. Schott, R. Juge, V. Krizáková, M. Belmeguenai, Y. Roussigné, A. Bernard-Mantel, L. Ranno, S. Pizzini, S.-M. Chérif, A. Stashkevich, S. Auffret, O. Boulle, G. Gaudin, M. Chshiev, C. Baraduc, and H. Béa, "Large-voltage tuning of Dzyaloshinskii–Moriya interactions: A route toward dynamic control of skyrmion chirality," *Nano Lett.* **18**, 4871–4877 (2018).
- 5L. Herrera Diez, Y. Liu, D. Gilbert, M. Belmeguenai, J. Vogel, S. Pizzini, E. Martinez, A. Lamperti, J. Mohammedi, A. Laborieux, Y. Roussigné, A. Grutter, E. Arenholtz, P. Quarterman, B. Maranville, S. Ono, M. S. E. Hadri, R. Tolley, E. Fullerton, L. Sanchez-Tejerina, A. Stashkevich, S. Chérif, A. Kent, D. Querlioz, J. Langer, B. Ocker, and D. Ravelosona, "Nonvolatile ionic modification of the Dzyaloshinskii–Moriya interaction," *Phys. Rev. Appl.* **12**, 034005 (2019).
- 6R. Pachat, D. Ourdani, J. van der Jagt, M.-A. Syskaki, A. Di Pietro, Y. Roussigné, S. Ono, M. Gabor, M. Chérif, G. Durin, J. Langer, M. Belmeguenai, D. Ravelosona, and L. H. Diez, "Multiple magnetoionic regimes in  $\text{Ta/Co}_{20}\text{Fe}_{60}\text{B}_{20}/\text{HfO}_2$ ," *Phys. Rev. Appl.* **15**, 064055 (2021).
- 7R. Pachat, D. Ourdani, M.-A. Syskaki, A. Lamperti, S. Roy, S. Chen, A. D. Pietro, L. Largeau, R. Juge, M. Massouras, C. Balan, J. W. van der Jagt, G. Agnus, Y. Roussigné, M. Gabor, S. M. Chérif, G. Durin, S. Ono, J. Langer, D. Querlioz, D. Ravelosona, M. Belmeguenai, and L. H. Diez, "Magneto-ionics in annealed  $\text{W/CoFeB/HfO}_2$  thin films," *Adv. Mater. Interfaces* **9**, 2200690 (2022).
- 8C.-E. Fillion, J. Fischer, R. Kumar, A. Fassatoui, S. Pizzini, L. Ranno, D. Ourdani, M. Belmeguenai, Y. Roussigné, S.-M. Chérif, S. Auffret, I. Joumard, O. Boulle, G. Gaudin, L. Buda-Prejbeanu, C. Baraduc, and H. Béa, "Gate-controlled skyrmion and domain wall chirality," *Nat. Commun.* **13**, 5257 (2022).
- 9Y. Guan, X. Zhou, F. Li, T. Ma, S.-H. Yang, and S. S. P. Parkin, "Ionitronic manipulation of current-induced domain wall motion in synthetic antiferromagnets," *Nat. Commun.* **12**, 5002 (2021).
- 10M. Huang, M. U. Hasan, K. Klyukin, D. Zhang, D. Lyu, P. Gargiani, M. Valvidares, S. Sheffels, A. Churikova, F. Büttner, J. Zehner, L. Caretta, K.-Y. Lee, J. Chang, J.-P. Wang, K. Leistner, B. Yildiz, and G. S. D. Beach, "Voltage control of ferrimagnetic order and voltage-assisted writing of ferrimagnetic spin textures," *Nat. Nanotechnol.* **16**, 981–988 (2021).
- 11A. Fassatoui, J. P. Garcia, L. Ranno, J. Vogel, A. Bernard-Mantel, H. Béa, S. Pizzini, and S. Pizzini, "Reversible and irreversible voltage manipulation of interfacial magnetic anisotropy in  $\text{Pt/Co/oxide}$  multilayers," *Phys. Rev. Appl.* **14**, 064041 (2020).

- <sup>12</sup>Y. Guan, X. Zhou, T. Ma, R. Blasing, H. Deniz, S.-H. Yang, and S. S. P. Parkin, "Increased efficiency of current-induced motion of chiral domain walls by interface engineering," *Adv. Mater.* **33**, 2007991 (2021).
- <sup>13</sup>H. Almasi, M. Xu, Y. Xu, T. Newhouse-Illige, and W. G. Wang, "Effect of Mo insertion layers on the magnetoresistance and perpendicular magnetic anisotropy in Ta/CoFeB/MgO junctions," *Appl. Phys. Lett.* **109**, 032401 (2016).
- <sup>14</sup>B. Seng, D. Schönke, J. Yeste, R. M. Reeve, N. Kerber, D. Lacour, J.-L. Bello, N. Bergéard, F. Kammerbauer, M. Bhukta, T. Ferté, C. Boeglin, F. Radu, R. Abrudan, T. Kachel, S. Mangin, M. Hehn, and M. Kläui, "Direct imaging of chiral domain walls and Néel-type skyrmionium in ferrimagnetic alloys," *Adv. Funct. Mater.* **31**, 2102307 (2021).
- <sup>15</sup>S. Ikeda, K. Miura, H. Yamamoto, K. Mizunuma, H. D. Gan, M. Endo, S. Kanai, J. Hayakawa, F. Matsukura, and H. Ohno, "A perpendicular-anisotropy CoFeB–MgO magnetic tunnel junction," *Nat. Mater.* **9**, 721–724 (2010).
- <sup>16</sup>S. Ono, S. Seki, R. Hirahara, Y. Tominari, and J. Takeya, "High-mobility, low-power, and fast-switching organic field-effect transistors with ionic liquids," *Appl. Phys. Lett.* **92**, 103313 (2008).
- <sup>17</sup>H. Honjo, S. Ikeda, H. Sato, K. Nishioka, T. Watanabe, S. Miura, T. Nasuno, Y. Noguchi, M. Yasuhira, T. Tanigawa, H. Koike, H. Inoue, M. Muraguchi, M. Niwa, H. Ohno, and T. Endoh, "Impact of tungsten sputtering condition on magnetic and transport properties of double-MgO magnetic tunneling junction with CoFeB/W/CoFeB free layer," *IEEE Trans. Magn.* **53**, 17282719 (2017).
- <sup>18</sup>S. K. Li, X. T. Zhao, W. Liu, Y. H. Song, L. Liu, X. G. Zhao, and Z. D. Zhang, "Interface effect of ultrathin W layer on spin-orbit torque in Ta/W/CoFeB multilayers," *Appl. Phys. Lett.* **114**, 082402 (2019).
- <sup>19</sup>D. A. Gilbert, A. J. Grutter, E. Arenholz, K. Liu, B. J. Kirby, J. A. Borchers, and B. B. Maranville, "Structural and magnetic depth profiles of magnetonic heterostructures beyond the interface limit," *Nat. Commun.* **7**, 12264 (2016).